White Paper

Ultrasound Micro-Angiography (UMA) in the Prostate, Thyroid, and Breast

Pavlos S. Zoumpoulis, MD, PhD, Radiologist
Diagnostic Echotomography SA, 317 Kifissias Ave., GR 14561, Athens, Greece

May 2024

mindray
healthcare within reach

Introduction

Aim of this White Paper is to discuss the value of the Ultrasound Micro-Angiography (UMA) feature available in Mindray Ultrasound (US) systems and provide clinicians with a guide on its use on the Prostate, Thyroid, and Breast. This document does not replace the Color Doppler Guidelines found in the literature [1] but serves as a guide for Mindray US system UMA users.

Angiography for Diagnostic Purposes

Angiography is a medical imaging technique used for blood vessel lumen visualization. It mainly involves hemodynamic information visualization concerning arteries, veins, and heart chambers. Angiography is useful in clinical conditions related to blood flow, its direction, and tissue perfusion, such as Coronal Disease, Portal Hypertension, Macula Lutea, advanced diabetes and malignant tumors.

Ultrasound Angiography

Ultrasound Angiography is a non-invasive, radiation-free examination that uses Ultrasound Doppler techniques to visualize vessel hemodynamics. Color Doppler provides accurate information concerning blood flow direction and mean velocity. Conventional color Doppler applications may be limited from the aliasing effect, angle dependency, and reduced low flow sensitivity. Power Doppler applications provide density and red blood cells power information, mainly used for small vessel low flow visualization [2]. Spectral Doppler is a Fast Fourier Transformation application, which provides a graphical visualization of flow velocity over time. Ultrasound angiography is useful in clinical fields like Carotid Arteries, Mesenteric Vessels, Peripheral Arteries, Veins, and Tumors.

Ultrasound Micro-Angiography

Ultra-micro-angiography (UMA) is a Doppler technique aiming to improve vessel identification. It is characterized by enhanced sensitivity for low-velocity blood flow visualization. Conventional Color Doppler applications utilize focused waves and cannot typically distinguish signals from slow-moving tissue and blood flow, which reduces their performance in detecting micro-vessels. UMA technology, on the other hand, uses plane and divergent waves allowing faster sampling rate and, therefore, improved sensitivity. Moreover, a wall-filtering algorithm allows precise distinction of low-speed blood flow from low-speed tissue movement, therefore, accurately displaying micro-vessels. UMA may, hence, improve Color Doppler diagnostic performance for diseases characterized by micro-vascularization or angiogenesis (i.e., malignant neoplasms) [3].

The UMA feature includes three sub-modes, cUMA, pUMA, and sUMA. cUMA simultaneously visualizes the B-Mode and color information for low-velocity micro-vessels. pUMA displays Power Doppler information and has a directional option. sUMA provides high spatial resolution visualization of micro-vessels and allows the examiner to adjust background transparency (grades 0-4). Grade 0 only displays vasculature information, while grade 4 displays both vascular and B-Mode information with the brightest B-Mode setting. Even though the sUMA sub-mode is the most sensitive and may visualize the smallest vessels with slow velocity blood flow, it does not provide blood flow direction information as the cUMA and pUMA sub-modes. The UMA feature may be combined with the Glazing Flow feature to provide a 3D view of vessels leading to a more detailed visualization. Moreover, UMA allows vessel detectability quantification through Color Pixel Percentage (CPP).

The UMA feature provides additional hemodynamic diagnostic information in the Prostate, Thyroid, and Breast. Vascularization and neo-angiogenesis are crucial diagnostic findings that are more reliably visualized through UMA, which provides holistic imaging for both arteries and veins, leading to differential benign/malignant diagnosis.

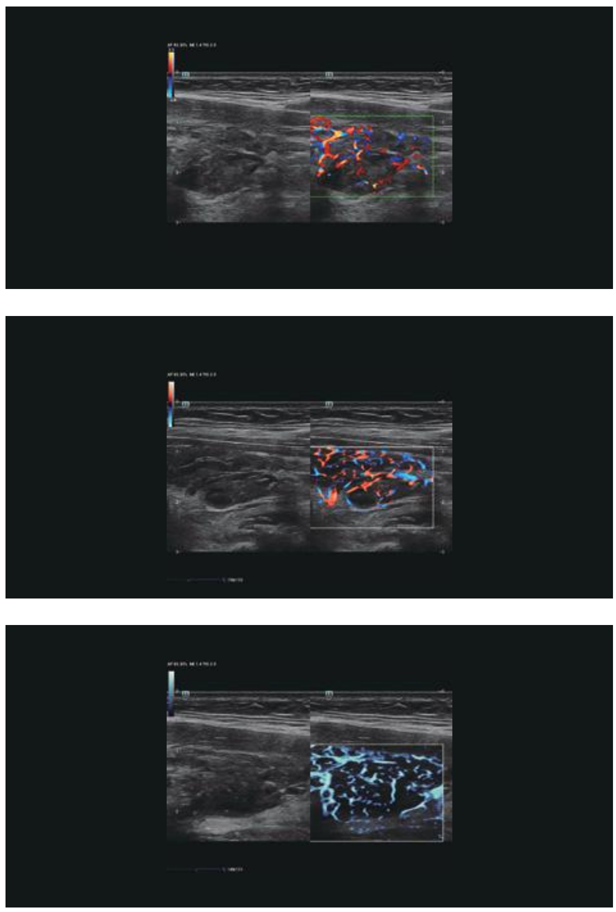

Figure1: Thyroid benign hyper-vascular adenomatous nodule visualized by the cUMA, pUMA and sUMA sub-modes.

Prostate

In 2020, Prostate Cancer (PrCa) was the second most common Cancer and the fifth most prominent cause of death for males all around the world [4]. Moreover, it was the most frequent cancer type in the United States in 2023 [5].

Transrectal or Transperineal Prostate biopsy, guided by Transrectal Ultrasound (TRUS) is considered the reference standard for PrCa diagnosis [6]. Despite TRUS strengths, which include availability, cost-effectiveness, familiarity to urologists, and real-time guidance, TRUS alone cannot reliably detect PrCa [7]. Methods such as Ultrasound Doppler, Elastography, CEUS and Multiparametric Ultrasound may contribute to PrCa detection by providing additional diagnostic information [8-20].

Prostate Hemodynamics

The Prostate and bladder share blood supply due to their anatomical proximity. Specifically, blood supply is mainly provided to the Prostate through the inferior vesical artery but also from the middle rectal and internal pudendal arteries [21]. Veins located around the Prostate compose the prostatic plexus which drains into the internal iliac veins. The Prostate gland also drains to the internal iliac lymph nodes and the sacral lymph nodes.

Color Doppler in the Prostate

Differentiating PrCa from normal prostatic parenchyma through Ultrasound B-Mode is often challenging because normal and neoplastic parenchyma may have similar echostrucure [22]. Moreover, tumors in the TZ are very challenging to visualize through B-Mode.

Color Doppler applications can play a role in PrCa diagnosis by identifying and characterizing the vascularity of suspicious lesions [8]. Specifically, Power and Color Doppler can visualize the flow patterns commonly encountered in PrCas: diffuse flow within the lesion, the most common pattern, focal flow within the lesion, or flow surrounding the lesion [23]. Even though Color Doppler may improve the TRUS sensitivity and diagnostic performance for detecting PrCas, it does not improve specificity [24]. This occurs due to cases of Prostate Inflammation (i.e., prostatitis) that can be commonly confused with malignant lesions if no complementary clinical information is available [25, 26]. Color Doppler in the Prostate is limited by operator dependency and lack of standardization [27].

UMA added value in the Prostate

UMA can partly solve the limitations of Color Doppler in the Prostate due to its increased sensitivity. Specifically, normal PZ vessels' entire trajectory is visible through UMA. This is not the case in the TZ, where TRUS is generally limited due to hyperplasia and infections. Moreover, in PZ tumors, which are located close to the transducer, UMA allows a very precise visualization of the lesion' s vasculature, including the characteristic of PrCa, neo-plastic vessels.

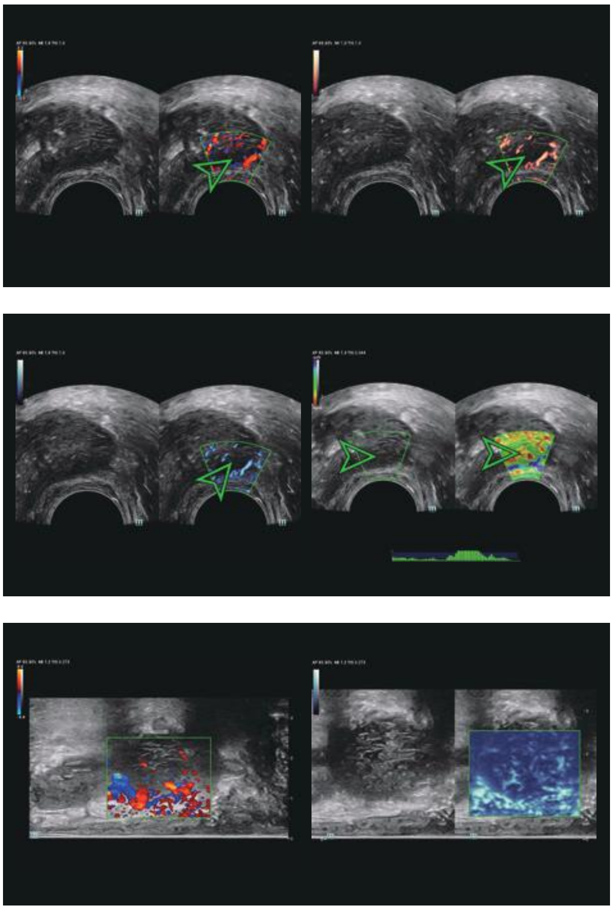

Figure 2: Typical hypo-echoic, hyper-vascular adenocarcinoma in the left PZ, visualized by the cUMA, sUMA, pUMA sub-modes, using both an Endfire and a Bi-plane transducer. The adenocarcinoma is stiffer than the surrounding PZ parenchyma in Elastography. Green arrow Adenocarcinoma

Thyroid

The most common Ultrasound Thyroid cancer risk classification tool is the Thyroid Imaging-Reporting and Data System (TIRADS). EU-TIRADS is the latest reporting system provided by the European Thyroid Association, used for Ultrasound thyroid nodule assessment. It involves assessing echogenicity, shape, margin, and micro-calcifications. Even though hemodynamic features are not evaluated for the TIRADS classification system, Color/Power Doppler and UMA can provide additional hemodynamic diagnostic information, especially for benign/malignant differentiation.

Thyroid Anatomy and Hemodynamics:

The Thyroid gland is an organ consisted of two lobes, which are connected through a narrow tissue band, the isthmus. Thyroid blood supply is provided by the superior Thyroid artery, the inferior Thyroid artery, and sometimes by the Thyroid ima artery [28, 29]. The superior Thyroid artery splits into the anterior and posterior branches while the inferior Thyroid artery splits into the superior and inferior branches [28]. The superior and inferior Thyroid arteries then merge behind the inferior pole of the Thyroid [29]. Blood is drained from the Thyroid through the superior and middle Thyroid veins, which drain to the internal jugular vein [28, 29]. Thyroid vessels described above develop a network between the two layers of the Thyroid capsule [29].

Color Doppler in the Thyroid:

Ultrasound Doppler applications, including spectral Doppler, Color Doppler, power Doppler, have a role to play in Thyroid Ultrasound examinations [31-42]. Specifically, Color Doppler contributes to the differential diagnosis of thyroid nodules, metastatic cervical lymph nodes, and diffuse parenchymal disease [30]. Moreover, Color Doppler contributes to US guided procedure guidance (i.e., Fine Needle Aspiration).

Color Doppler applications contribute to Thyroid nodule characterization through vascularity pattern visualization. Specifically, Thyroid nodule vascularity patterns are categorized into the following types. Type 1 is characterized by no vascularity, while type 2 nodules present peri-nodular vascularity. Type 3 nodules have mild (<50%) intra-nodular vascularity and, finally, type 4 nodules have increased (>50%) intra-nodular vascularity [37]. Color Doppler Ultrasound applications are commonly used for benign-malignant nodule differentiation and are characterized by high sensitivity and specificity, as well as by acceptable diagnostic performance [43-48]. Increased intra-nodular anarchic vascularity is considered pathognomonic for Thyroid nodule malignancy [43-48].

Power Doppler improves benign-malignant nodule differentiation through increased sensitivity in detecting small vessel slow blood flow [49-52]. UMA further increases sensitivity of small vessel slow blood flow detection.

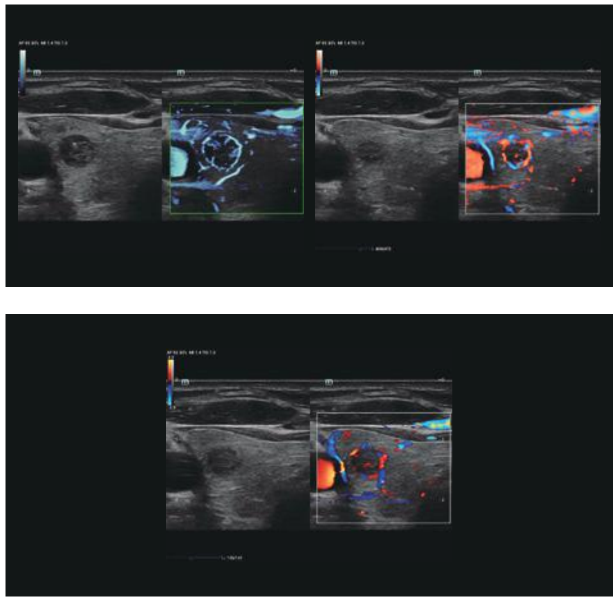

Figure 3: Typical Thyroid benign hypo-echoic adenomatous nodule, hyper-vascular mainly in the periphery, visualized by the sUMA, pUMA and cUMA sub-modes.

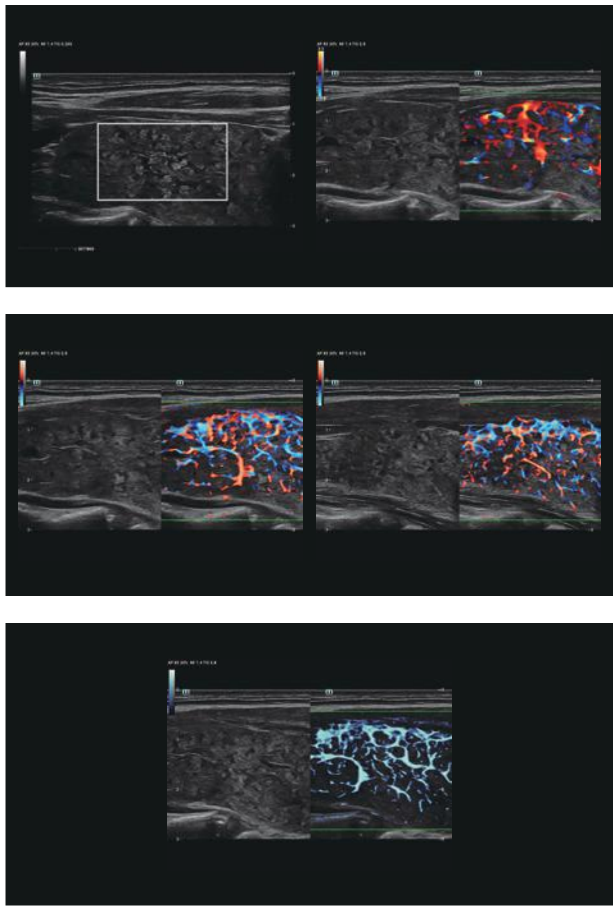

Figure 4: Typical auto-immune hyper-vascular thyroiditis in the acute phase, visualized by the cUMA, pUMA, and sUMA sub-modes. All vessels are normal and diverted.

UMA added value in the Thyroid

UMA may visualize peri-nodular and intra-nodular thyroid microvascular flow more reliably and in greater detail than conventional Color Doppler applications. Since increased vasculature and intra-nodular flow are linked with Thyroid nodule malignancy, UMA can increase the accuracy of Ultrasound examinations in malignant Thyroid nodule assessment. Formation of new vessels characterizes the development of all Thyroid malignant neoplasms. Neo-vessels present stenoses, dilatations and arterio-venous anastomoses. It is, therefore, vital to visualize very slow flow vessels, which may be accomplished through UMA. Moreover, through UMA the visualization of the irregular neo-vessels' wall is possible, due to the absence of artefacts (flow exceeding the borders of the vessels).

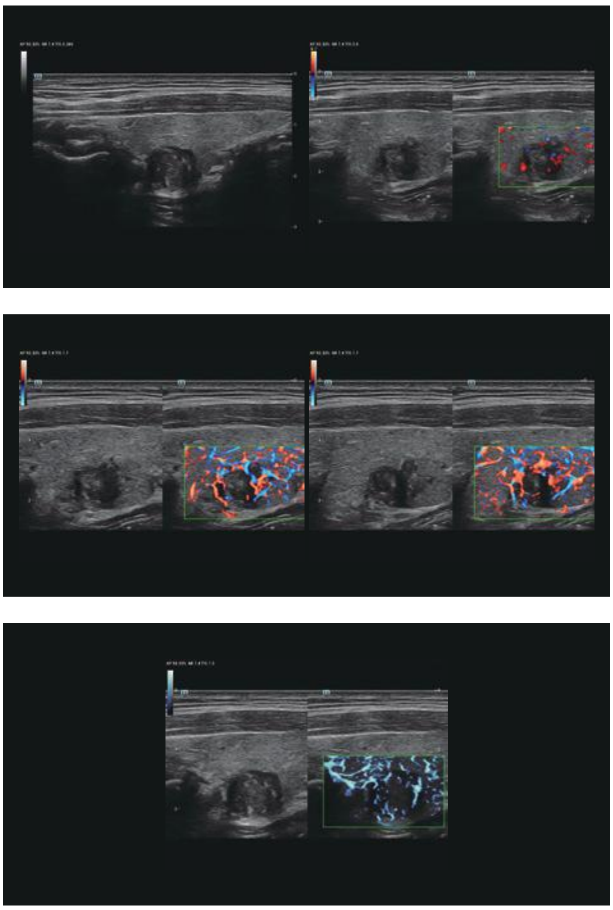

Figure 5: Typical heterogeneous, mainly hypo-echoic, Thyroid papillary carcinoma. The carcinoma is hyper-vascular with neo-plastic vessels both in its periphery and within its borders.

Breast

The Breast Imaging-Reporting and Data System (BIRADS) is a risk classification tool developed by American College of Radiology, used for Breast tumor assessment. BIRADS is a seven-stage scale used for Ultrasound, as well as for mammography and MRI. It evaluates morphological features, such as tissue composition, masses information, and calcifications. Even though hemodynamic features are not evaluated for BIRADS classification system, Color/Power Doppler and UMA can provide additional hemodynamic diagnostic information, especially for benign/malignant differentiation.

Color Doppler for Breast Screening and Diagnosis

Color Doppler may distinguish complicated/hemorrhagic cysts from anechoic malignant lesions, such as medullary carcinomas and metastases. Moreover, it may differentiate intra-cystic, intraductal debris and apocrine metaplasia from solid tissue, such as papillary lesions and intraductal carcinomas [53]. Furthermore, Color Doppler can assess if lymphadenopathy occurs due to inflammation, metastatic Breast carcinoma, or lymphoma and can demonstrate inflammatory hyperemia (i.e., in mastitis). The differentiation between inflammatory and metastatic enlarged lymph nodes is challenging to accomplish through Hemodynamic information alone.

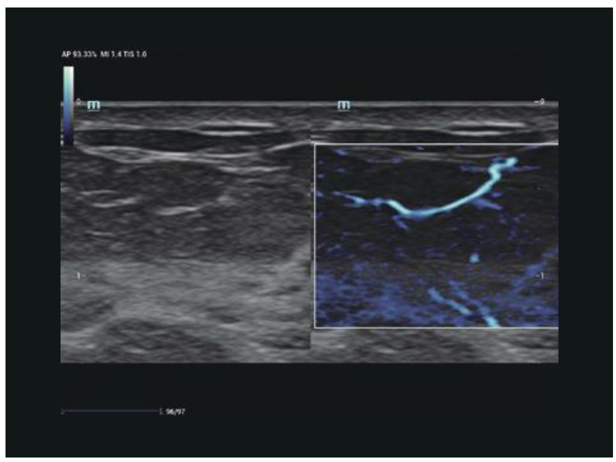

Figure 6: Normal Breast echo-structure and normal vessels visualized by the sUMA sub-mode.

UMA for Breast Screening and Diagnosis

To effectively assess tumor hemodynamics, advanced Doppler techniques, like UMA, have been introduced, improving sensitivity for micro neo-plastic vessels, enhancing resolution, and reducing motion artefacts [54].

UMA may improve US diagnostic performance for Breast malignancy by reliably evaluating vessel complexity [55-59]. Effective and efficient use of UMA, however, requires training and knowledge of appropriate clinical application [54].

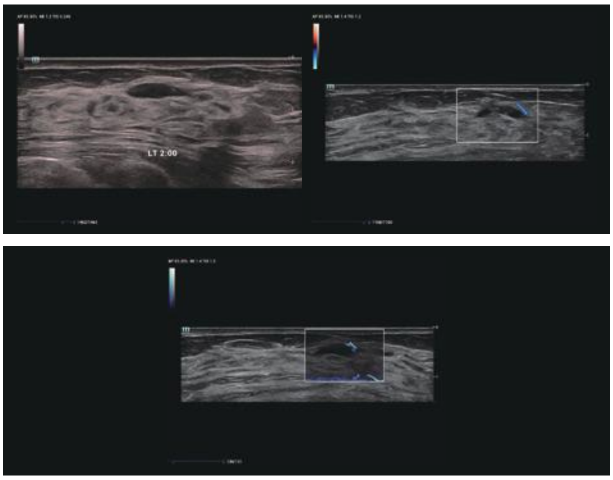

Figure 7: Typical hypo-echoic Breast fibro-adenoma with regular borders and normal vessels, visualized by the pUMA, and sUMA sub-modes.

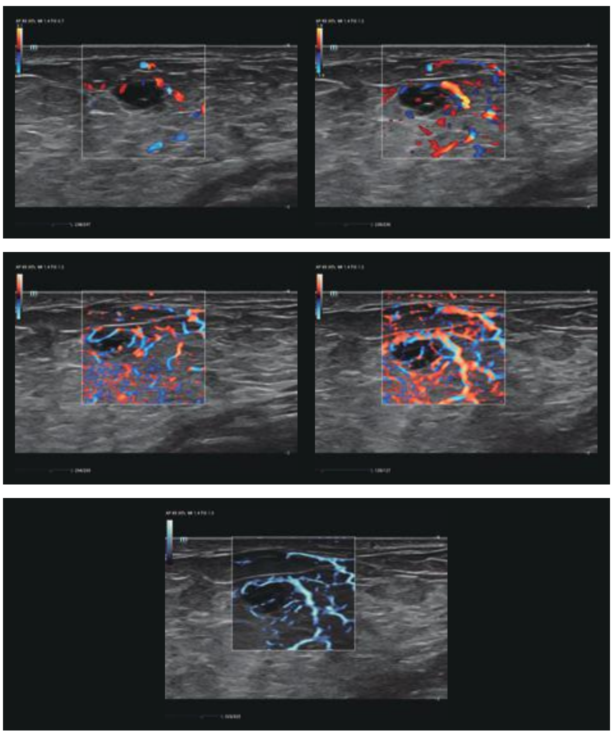

Figure 8: Cystic benign lesion with diaphragms and internal echogenic spots visualized by the pUMA, sUMA and cUMA sub-modes. Regular vessels in the perimeter of the cysts and throughout the septa/diaphragms. This benign vascularization is only visible through UMA and not through conventional Color Doppler.

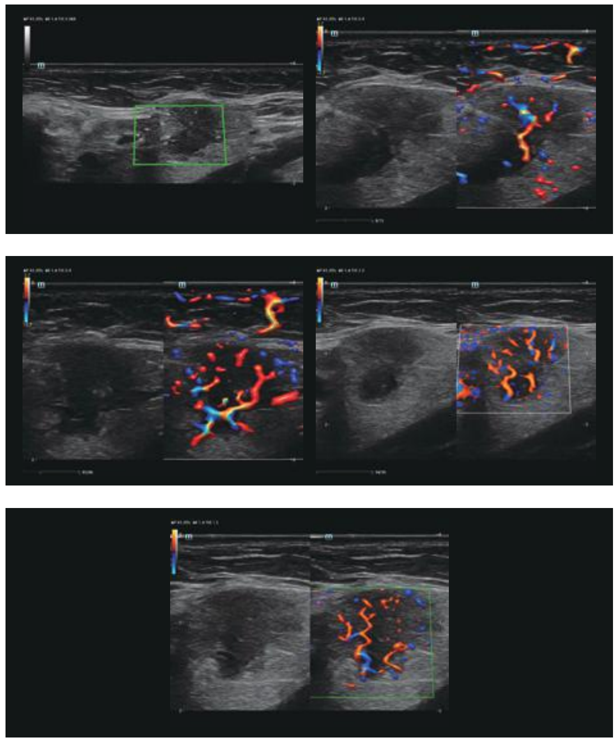

Figure 9: Typical hypo-echoic lobular Breast carcinoma. Some proximal and central micro calcifications are visible in B-Mode. The lesion invades the peri-tumoral fat. The lesion is hyper-vascular and neoplastic vessels are clearly visible in cUMA and pUMA sub-modes.

UMA step-by-step application

1.The probe should be as stable as possible during UMA examinations. The patient should be instructed to hold his/her breath

2.Locate the target lesion through B-Mode. Zoom when necessary and enable the UMA feature using the touchscreen

3.Adjust the UMA ROI to include the entire lesion and adjacent tissue

4.Switch between cUMA, pUMA, and sUMA sub-modes

5.Adjust frequency scale, gain and wall filter to acquire the optimum image quality and reduce motion artefacts

- Use as high frequency as possible without compromising US beam penetration. As frequency increases more micro-vessels may be detected
- In the pUMA and sUMA sub-modes reduced scale leads to increased sensitivity for low velocity vessels
- Increased wall filter frequency may reduce motion artefacts

Interesting UMA Cases

Prostate

Case 1

Prostate Cancer, 76-year-old male Patient

Clinical information: negative DRE

Imaging information: recent MRI examination reported PIRADS 4 lesions in the right PZ

Biochemical information: PSA 9 ngr, ratio 0.21

Ultrasound information: Hypoechoic, hyper-vascular and stiff in Elastography lesions in the right PZ in the middle and base of the gland

UMA information: The UMA feature can reliably visualize neo-vessels in both the periphery and inside the lesion. These neo-vessels present derivation, stenosis, dilatation, and occlusion

Histologic information: both lesions turned out to be Gleason 7 invasive adenocarcinoma

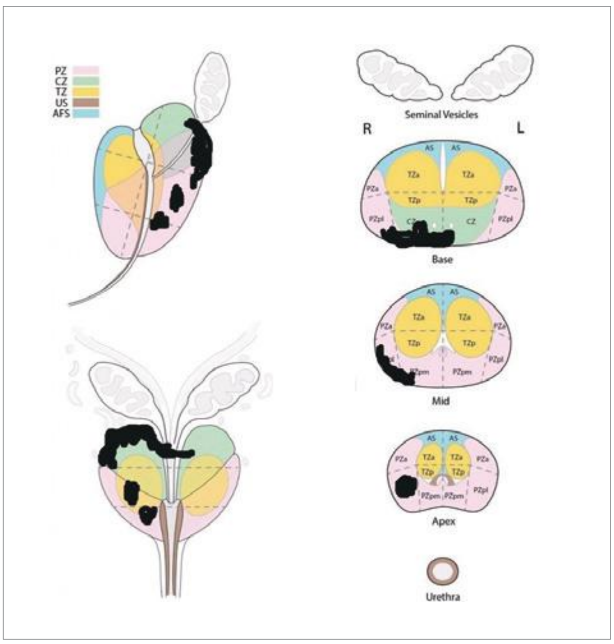

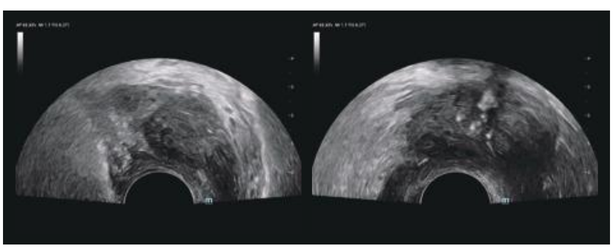

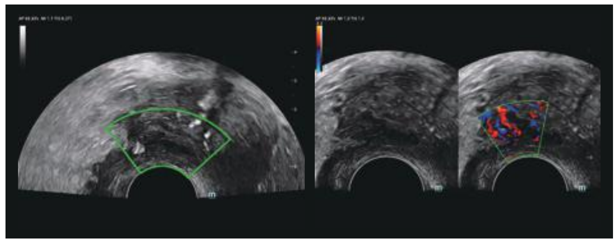

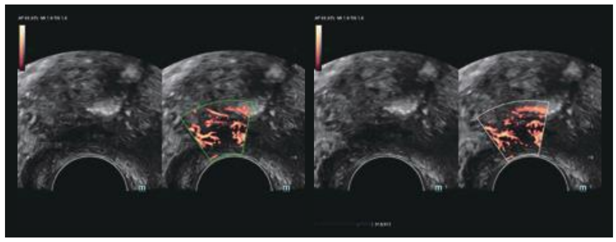

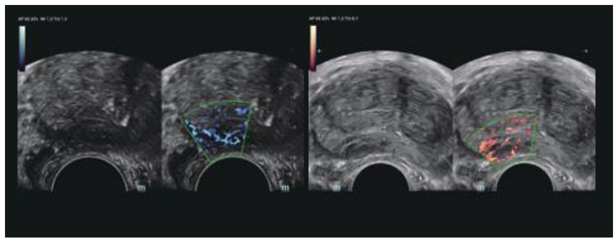

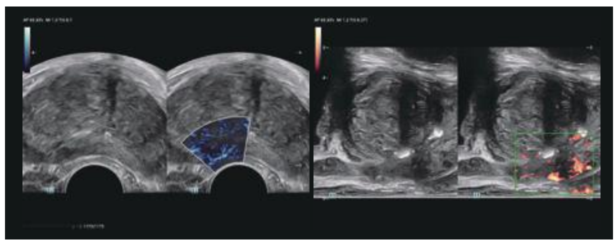

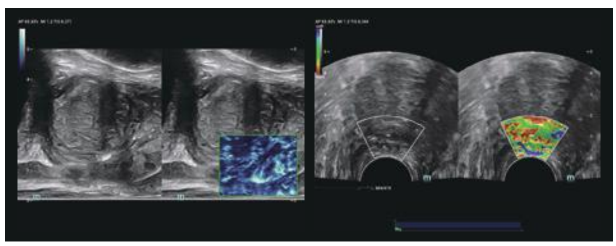

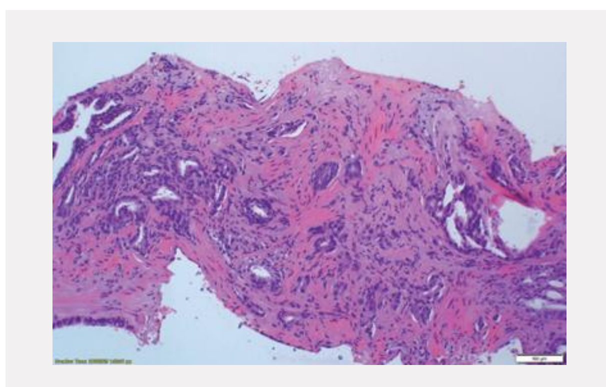

Case 2

Prostate Cancer, 77-year-old Male Patient

Clinical information: negative DRE

Imaging information: an MRI examination performed 5 years prior reported a PIRADS 4 lesion in the anterior PZ on the left. A Biopsy performed then came out negative

Biochemical information: PSA 13.6 ngr

Ultrasound information: Hypo- and hyper-echoic, hyper-vascular and s in the left PZ invading the TZ. Since the lesion invades the TZ is barely visible in TRUS

Elastography information: Lesion is stiff in Elastography. Elastography helps in visualizing lesions in the TZ and, therefore, helps in guiding the Prostate biopsies

UMA information: The UMA feature can reliably visualize tortuous neo-vessels mainly in the periphery of the lesion with stenoses and dilatations

Histologic information: the lesion turned out to be Gleason 6 invasive adenocarcinoma

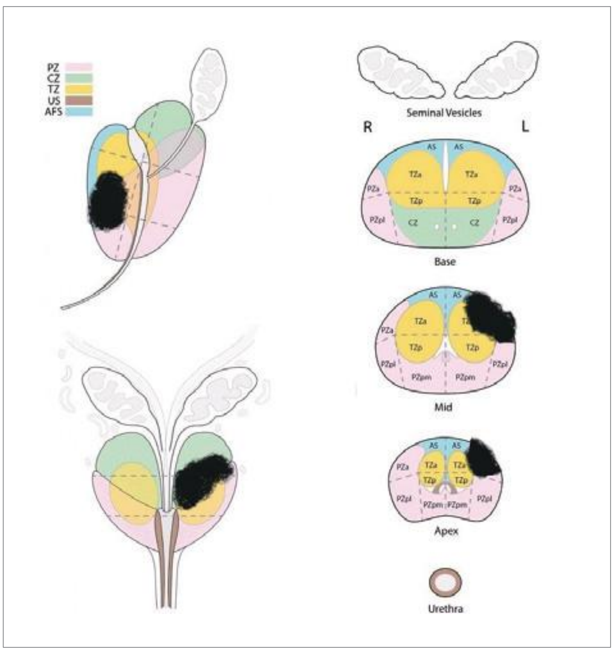

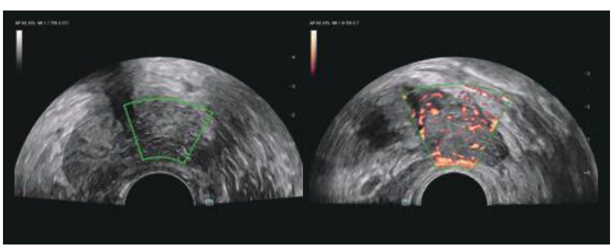

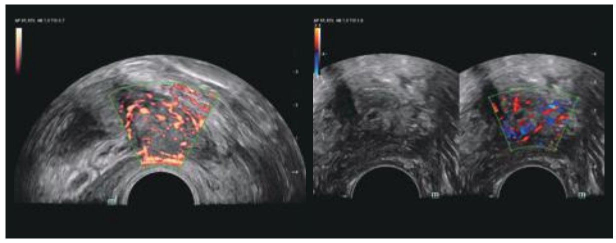

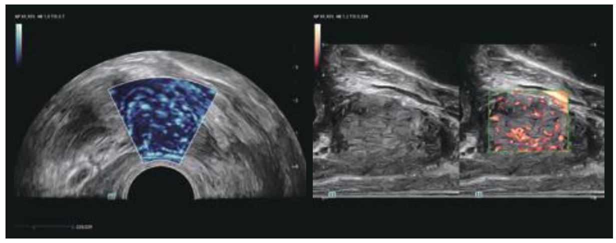

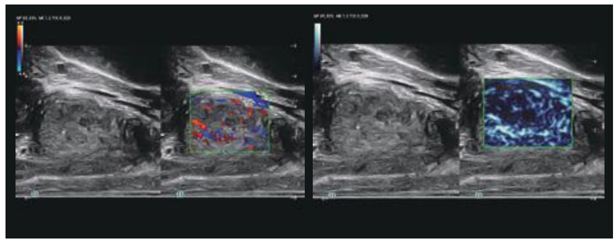

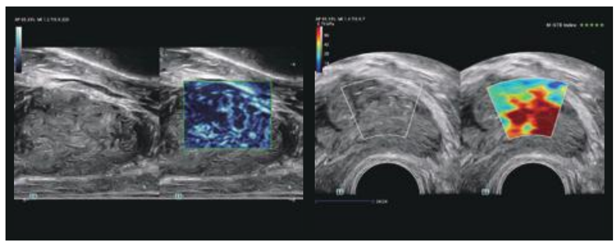

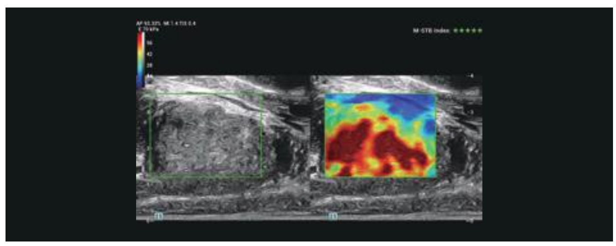

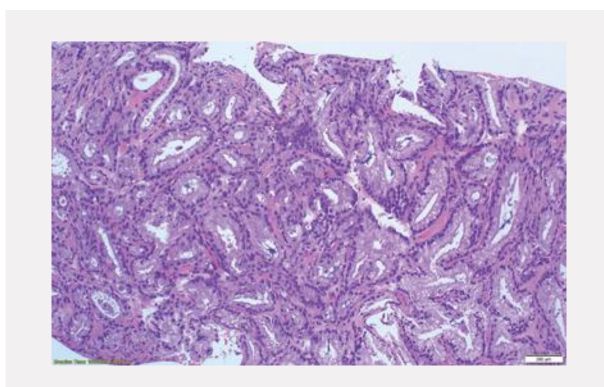

Case 3

Prostate Cancer, 60-year-old Male Patient

Clinical information: negative DRE

Imaging information: -

Biochemical information: PSA 7.35 ngr

Ultrasound information: Hypo-echoic, hyper-vascular, stiff in Elastography lesion in the right PZ

UMA information: Only the proximal part of the tumor is hypervascular, there is an abrupt interruption of blood flow, due to the tumor invasion

Histologic information: the lesion turned out to be Gleason 7 invasive adenocarcinoma

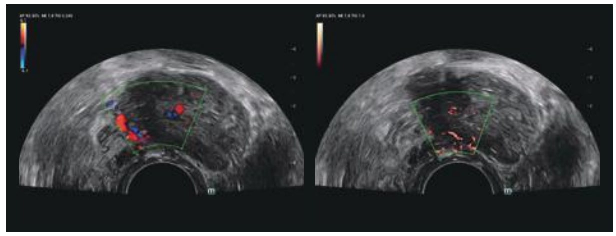

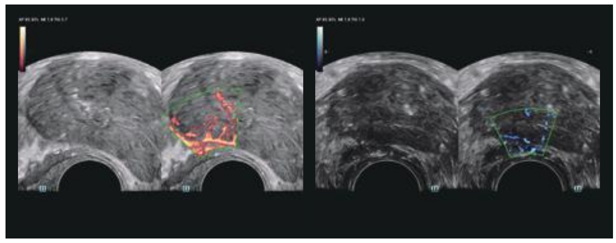

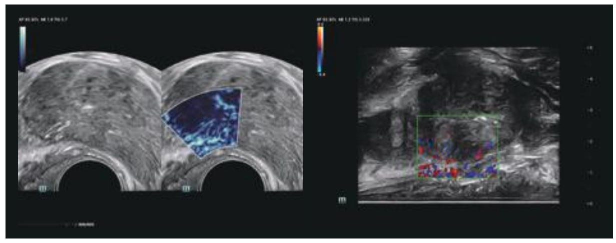

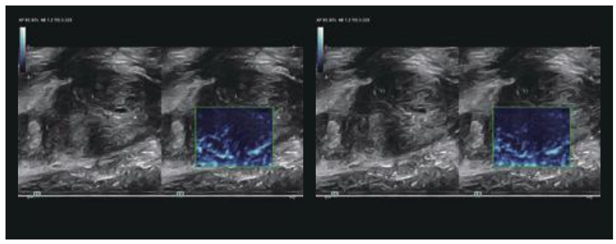

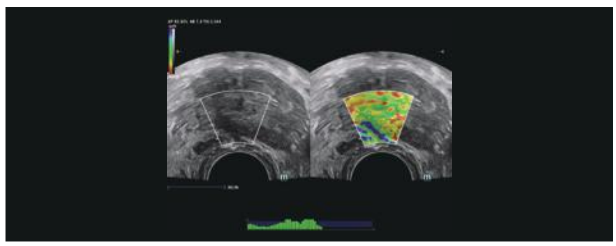

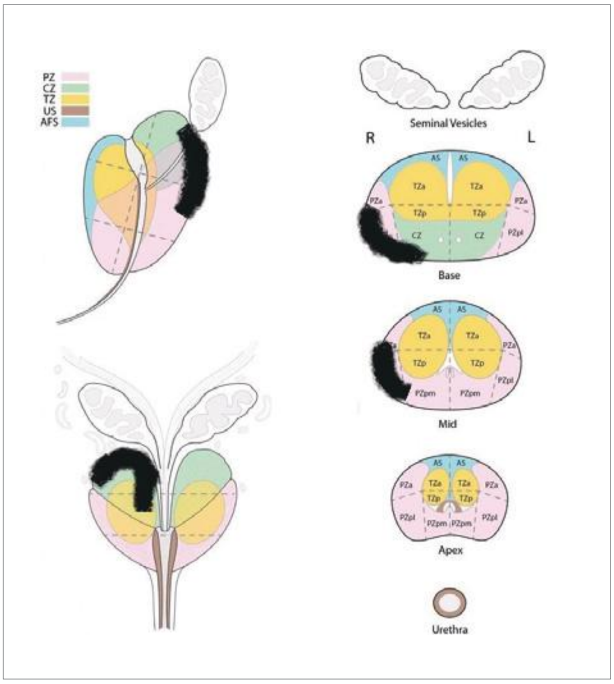

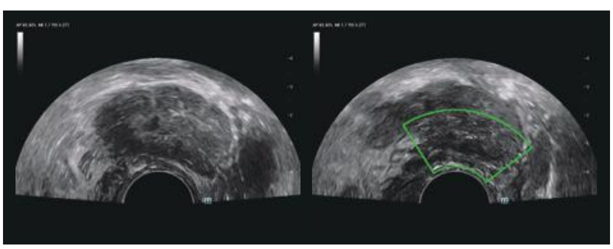

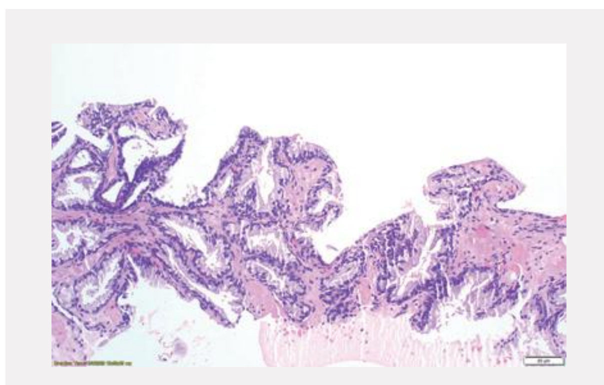

Case 4

Prostate Cancer, 82-year-old male Patient

Clinical information: no symptoms, negative DRE

Imaging information: a previous MRI examination mentioned a PIRADS 3 lesion in the apex

Biochemical information: PSA 10.3 ngr (recent PSA elevation)

Ultrasound information: hypo-echoic tumor in the PZ in the apex of the gland

UMA information: tortuous, stenotic, and abruptly interrupted neo-vessels, mainly in the periphery of the tumor

Elastography information: the lesion appears stiffer using both STE ("no-signal"/ dark blue) and Strain Elastography and both convex and linear transducers

Histologic information: the lesion turned out to be Gleason 8 invasive adenocarcinoma

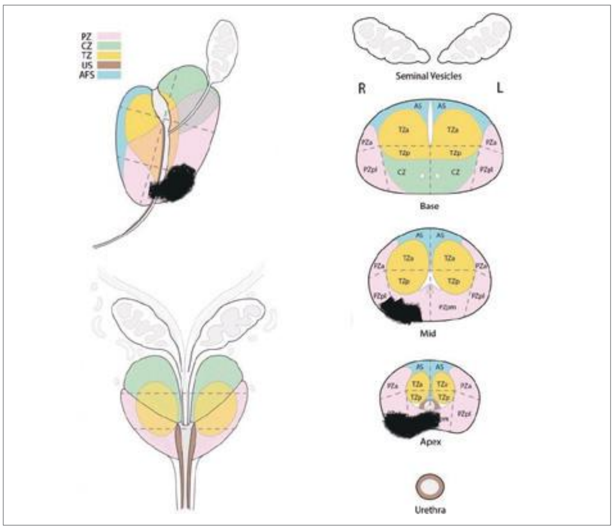

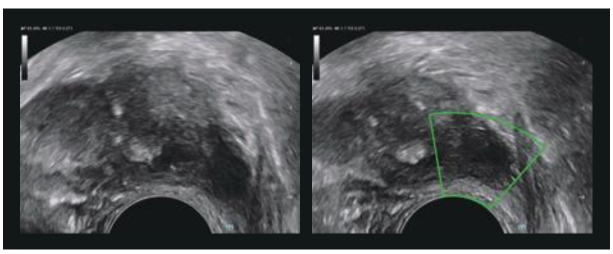

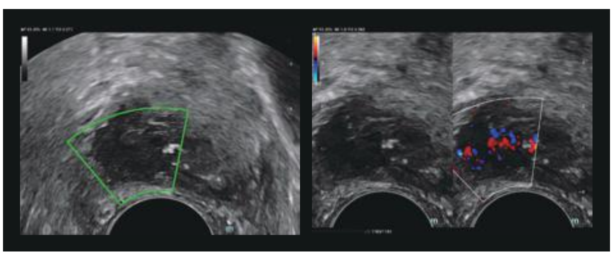

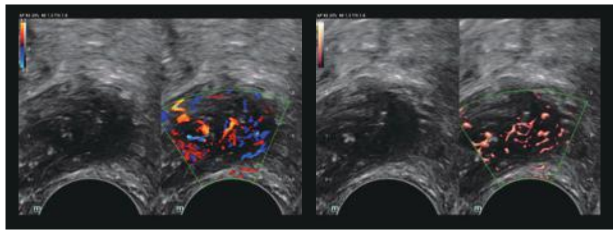

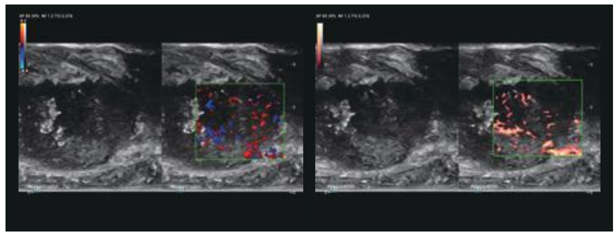

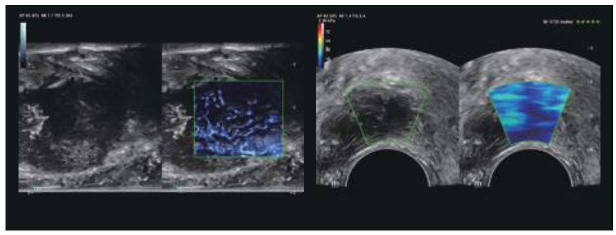

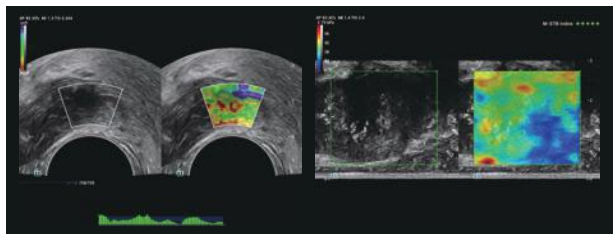

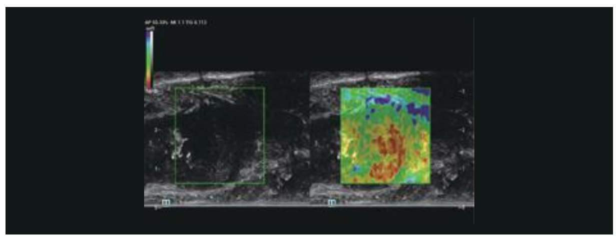

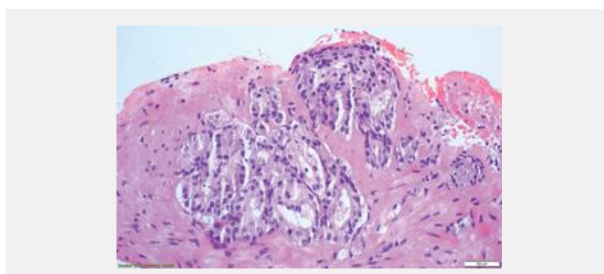

Thyroid

Case 1

Thyroid Nodule, 50-year-old female Patient

Clinical information: no symptoms

Biochemical information: no findings

Ultrasound information: normal volume Thyroid lobes, ovoid and round nodules containing liquid collections

Elastography information: no difference in elasticity measurements between nodule and parenchyma

UMA information: typical circular vascular network corresponding to the hypo-echoic halo comprised of normal vessels, normal linear or curved vessels within the nodule (no neo-vessels found)

Cytology information: benign hyperplastic nodule

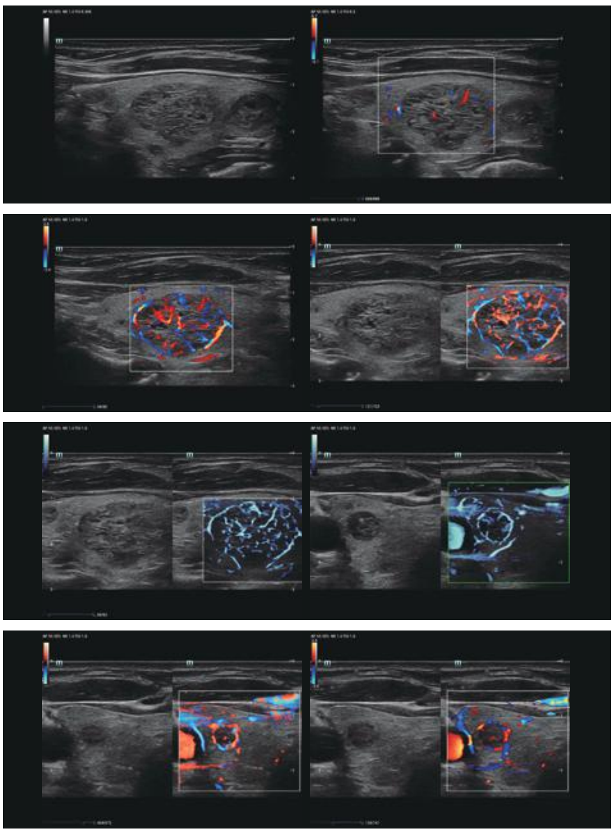

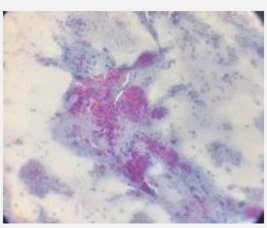

Case 2

Thyroid Cancer, 35-year-old male Patient

Clinical information: no symptoms

Biochemical information: no findings

Ultrasound information: hypo-echoic heterogeneous lesion with an iso-echoic component and irregular borders containing echogenic foci

Elastography information: part of the nodule is stiffer than the surrounding parenchyma

UMA information: no regular vessels in the lesion periphery, irregular internal neo-vascularization with dilatations, stenoses and occlusions

Cytology information: follicular carcinoma

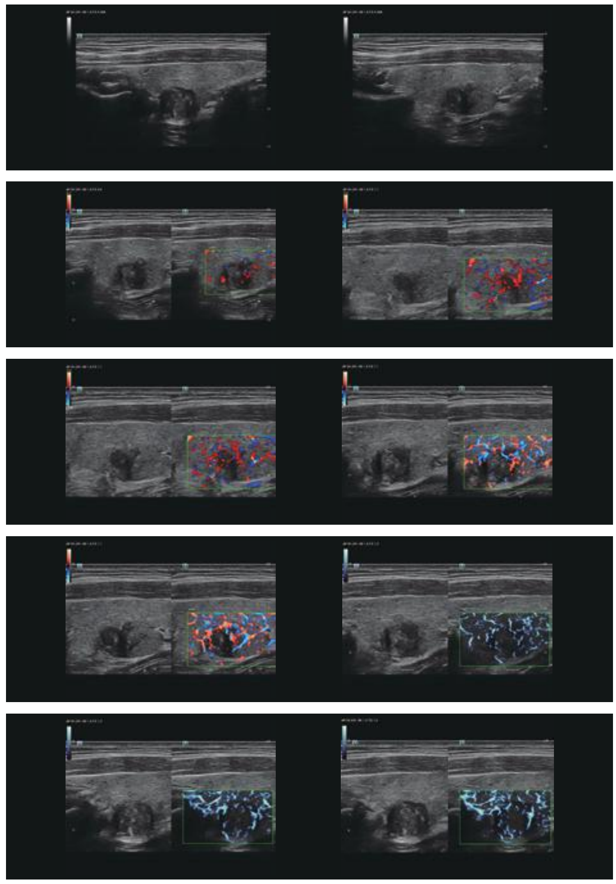

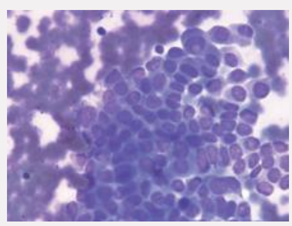

Case 3

Auto-immune Thyroiditis, 31-year-old male Patient

Clinical information: mild throat pain

Biochemical information: hypothyroidism, elevated anti-thyroid antibodies

Ultrasound information: augmented volume in both lobes, lobulations, coarse heterogeneity with small liquid collections

Cytology information: Hashimoto thyroiditis in acute phase

UMA information: diffuse hyper-vascularity, normal vessels in the parenchyma and I the pseudo-nodules, no vascular circular pattern

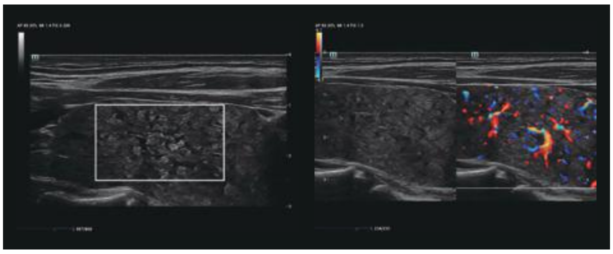

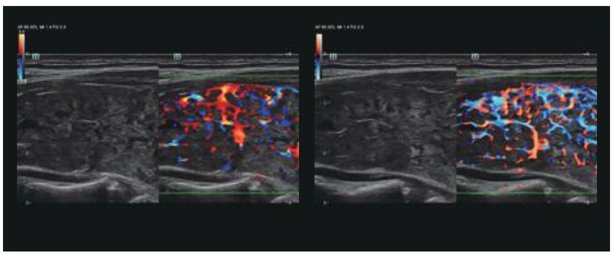

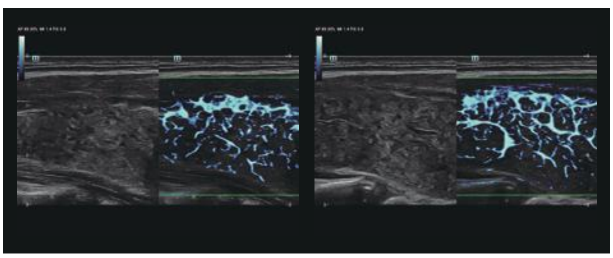

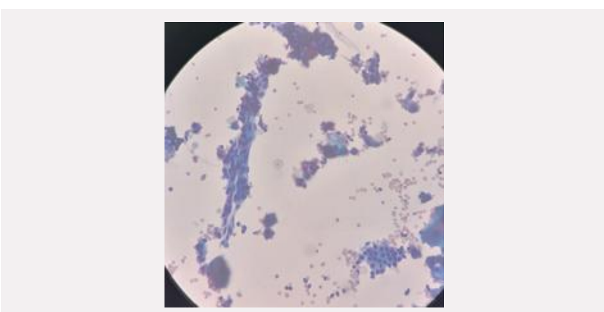

Breast

Case 1

Breast Fibroadenoma, 53-year-old female Patient

Clinical information: no symptoms

Imaging information: small regular subcutaneous lesion with a 0.9cm diameter in the right breast in a recent mammography

Ultrasound information: hypo- / an-echoic longitudinal lesion with regular (linear) borders

UMA information: both lesions are hypo-vascular, no internal vascularization, small regular vessels in the periphery. The feeding artery is visible

Histologic information: fibroadenoma

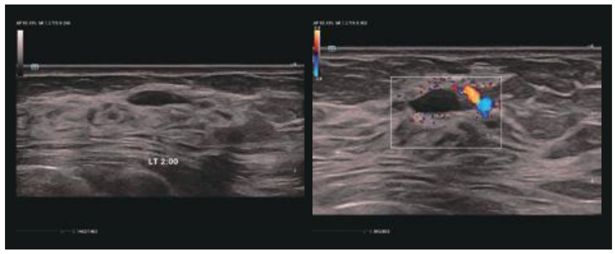

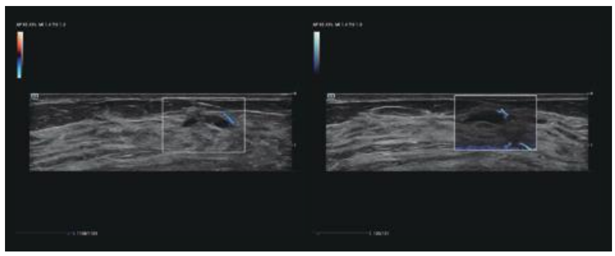

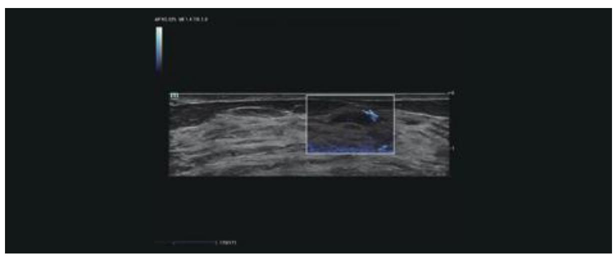

Case 2

Breast adenocarcinoma, 38-year-old female Patient

Clinical Information: no symptoms

Imaging information: previous mammography with no findings

Ultrasound information: solid hypo- and iso-echoic bilobular lesion in the right breast (2,1cm).

Elastography information: discreet increase of stiffness values in the hypoechoic part of the lesion

UMA information: its hypo-echoic part contains irregular neo-vessels with stenoses and dilatations

Histologic information: Breast adenocarcinoma

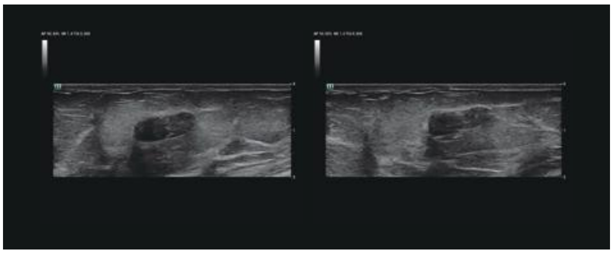

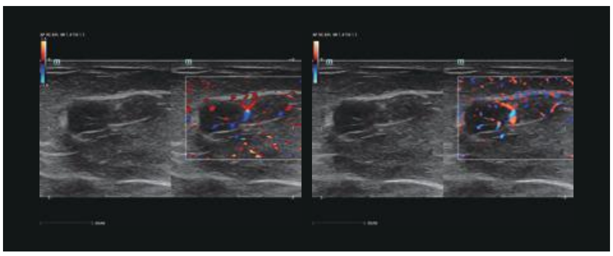

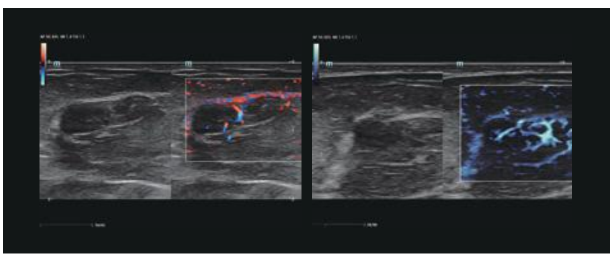

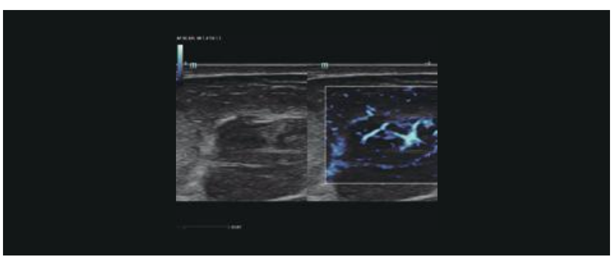

Case 3

Breast adenocarcinoma, 56-year-old female Patient

Clinical information: palpable lesion in the left Breast anterior and external quadrant.

Imaging information: irregular dense lesion with micro-calcifications in recent mammography

Ultrasound information: solid, lobular, spiculated lesion with irregular borders

Elastography information: lesion is stiffer than the surrounding parenchyma

UMA information: the entire lesion contains tortuous neoplastic vessels with both stenotic and dilated parts

Histologic information: Breast adenocarcinoma

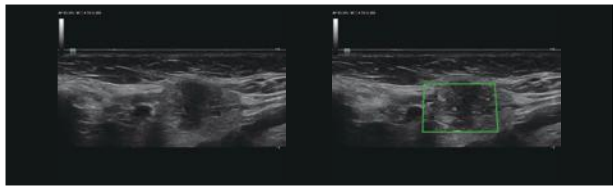

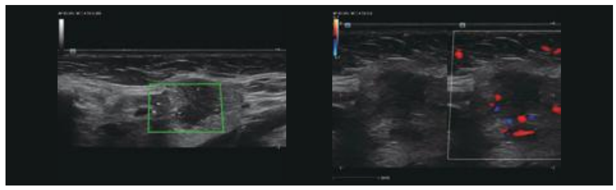

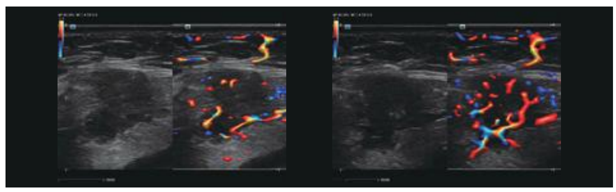

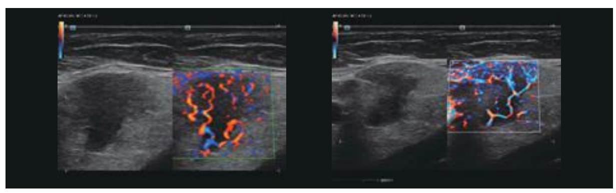

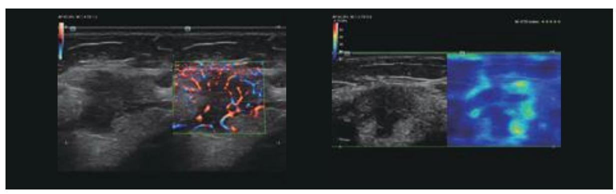

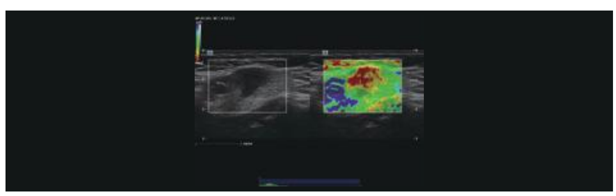

Case 4

Breast adenocarcinoma, 48-year-old female Patient

Clinical information: No symptoms, no palpable lesion

Imaging information: ovoid dense lesion in the right Breast upper and external quadrant

Ultrasound information: hypo-echoic ovoid lesion. Spiculations are radiating from the margins in some sections

Elastography information: Even though the lesion appears soft (deep blue) in STE, this is an artifact. In very stiff lesions this artifact can be diagnostic (no signal zone)

UMA information: the neoplastic vessels within the lesion are only visualized through UMA and mainly through the sUMA sub-mode. The vessels are tortuous with both stenosis and dilatations.

Histologic information: Breast adenocarcinoma

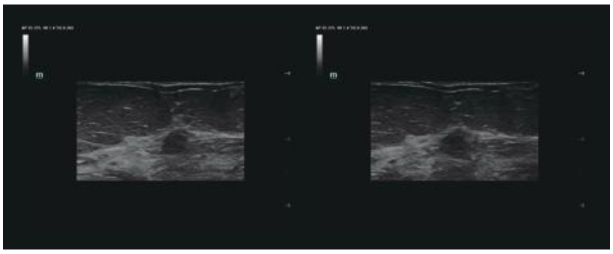

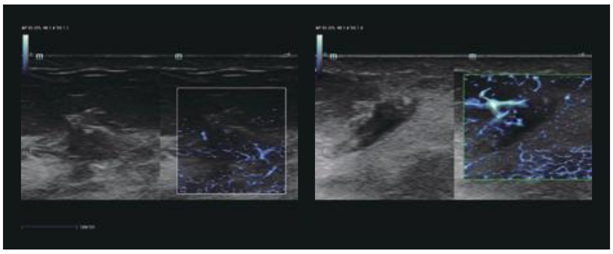

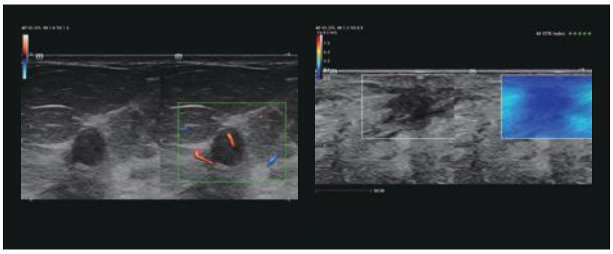

References

[1] Beyer-Enke, S.A., Mück-Weymann, M. (2000). Ultrasound Angiography. In: Zeitler, E. (eds) Radiology of Peripheral Vascular Diseases. Medical Radiology. Springer, Berlin, Heidelberg. https://doi.org/10.1007/978-3-642-56956-2_10

[2] Maulik, D. (2005). Spectral Doppler: Basic Principles and Instrumentation. In: Maulik, D. (eds) Doppler Ultrasound in Obstetrics and Gynecology. Springer, Berlin, Heidelberg. https://doi.org/10.1007/3-540-28903-8_3

[3] Zhao C, Wang Q, Wang M, Tao X, Liu S, Qi Z, Lanxi X, Liu D, He X, Tian X, Zeng X, Jiang Y, Yang M. Ultra-microangiography in evaluating the disease activity of rheumatoid arthritis and enhancing the efficacy of ultrasonography: A preliminary study. Eur J Radiol. 2021 Apr;137:109567. doi: 10.1016/j.ejrad.2021.109567. Epub 2021 Jan 26. PMID: 33556758.

[4] Sung H, Ferlay J, Siegel RL, et al. Global cancer statistics 2020: GLOBOCAN estimates of incidence and mortality worldwide for 36 cancers in 185 countries. CA Cancer J Clin 2021; 71: 209–249.

[5] Siegel, RL, Miller, KD, Wagle, NS, Jemal, A. Cancer statistics, 2023. CA Cancer J Clin. 2023; 73(1): 17-48. doi:10.3322/-caac.21763

[6] Cooperberg MR, Lubeck DP, Meng MV, et al. The changing face of low-risk prostate cancer: trends in clinical presentation and primary management. J Clin Oncol 2004; 22: 2141–2149.

[7] Smeenge M, Barentsz J, Cosgrove D, et al. Role of transrectal ultrasonography (TRUS) in focal therapy of prostate cancer: report from a consensus panel. BJU Int 2012; 110: 942–948.

[8] Ashi K, Kirkham B, Chauhan A, et al. Quantitative colour Doppler and greyscale ultrasound for evaluating prostate cancer. Ultrasound 2021; 29: 106–111.

[9] Glybochko PV, Alyaev YG, Amosov AV, et al. Evaluation of prostate HistoScanning as a method for targeted biopsy in routine practice. Eur Urol Focus 2019; 5: 179–185.

[10] Wildeboer RR, Postema AW, Demi L, et al. Multiparametric dynamic contrast-enhanced ultrasound imaging of prostate cancer. Eur Radiol 2017; 27: 3226–3234.

[11] Correas JM, Tissier AM, Khairoune A, et al. Prostate cancer: diagnostic performance of real-time shear-wave elastography. Radiology 2015; 275: 280–289.

[12] Lughezzani G, Saita A, Lazzeri M, et al. Comparison of the diagnostic accuracy of micro-ultrasound and magnetic resonance imaging/ultrasound fusion targeted biopsies for the diagnosis of clinically significant prostate cancer. Eur Urol Oncol 2019; 2: 329–332.

[13] Dias AB, O'Brien C, Correas J-M, et al. Multiparametric ultrasound and micro-ultrasound in prostate cancer: a comprehensive review. Br J Radiol 2022; 95: 20210633.

[14] Nelson ED, Slotoroff CB, Gomella LG, et al. Targeted biopsy of the prostate: the impact of color Doppler imaging and elastography on prostate cancer detection and Gleason score. Urology 2007; 70: 1136–1140.

[15] Xie SW, Li HL, Du J, et al. Contrast-enhanced ultrasonography with contrast-tuned imaging technology for the detection of prostate cancer: comparison with conventional ultrasonography. BJU Int 2012; 109: 1620–1626.

[16] Aigner F, Schäfer G, Steiner E, et al. Value of enhanced transrectal ultrasound targeted biopsy for prostate cancer diagnosis: a retrospective data analysis. World J Urol 2012; 30: 341–346.

[17] Brock M, Eggert T, Palisaar RJ, et al. Multiparametric ultrasound of the prostate: adding contrast enhanced ultrasound to real-time elastography to detect histopathologically confirmed cancer. J Urol 2013; 189: 93–98.

[18] Postema A, Mischi M, de la Rosette J, et al. Multiparametric ultrasound in the detection of prostate cancer: a systematic review. World J Urol 2015; 33: 1651–1659.

[19] Grey A, Ahmed HU. Multiparametric ultrasound in the diagnosis of prostate cancer. Curr Opin Urol 2016; 26: 114–119.

[20] Mottet N, Cornford P, van der Bergh R, et al. EAU-EANM-ESTRO-ESUR-SIOG guidelines on prostate cancer. European Association of Urology, 2022, https://d56bochluxqnz.cloudfront.net/documents/full-guideline/EAU-EANM-ESTRO-ESUR-ISUP_SIOG-Guidelines-on-Prostate-Cancer-2022_2022-04-25-063938_yfos.pdf (accessed 19 October 2022).

[21] Singh O, Bolla SR. Anatomy, Abdomen and Pelvis, Prostate. [Updated 2022 Jul 25]. In: StatPearls [Internet]. Treasure Island (FL): StatPearls Publishing; 2022 Jan-. Available from: https://www.ncbi.nlm.nih.gov/books/NBK540987/

[22] Correas JM, Halpern EJ, Barr RG, et al. Advanced ultrasound in the diagnosis of prostate cancer. World J Urol 2021; 39: 661–676.

[23] Chen FK, de Castro Abreu AL, Palmer SL. Utility of ultrasound in the diagnosis, treatment, and follow-up of prostate cancer: state of the art. J Nucl Med 2016; 57(Suppl. 3): 13S–18S.

[24] Kuligowska E, Barish MA, Fenlon HM, et al. Predictors of prostate carcinoma: accuracy of gray-scale and color Doppler US and serum markers. Radiology 2001; 220: 757–764.

[25] Sarıca Ö. Contribution of color Doppler sonography in the diagnosis of prostatic pathologies. South Clin Istanbul Eurasia 2019; 30: 255–260.

[26] Ukimura O, de Castro Abreu AL, Gill IS, et al. Image visibility of cancer to enhance targeting precision and spatial mapping biopsy for focal therapy of prostate cancer. BJU Int 2013; 111: E354–E364.

[27] Kaneko M, Lenon MSL, Storino Ramacciotti L, Medina LG, Sayegh AS, La Riva Rincon A, Perez LC, Ghoreifi A, Lizana M, Jadvar DS, Lebastchi AH, Cacciamani GE, Abreu AL. Multiparametric ultrasound of prostate: role in prostate cancer diagnosis. Ther Adv Urol. 2022 Dec 26;14:17562872221145625. doi: 10.1177/17562872221145625. PMID: 36601020; PMCID: PMC9806443.

[28] Standring S, Borley NR, et al., eds. (2008). Gray's anatomy: the anatomical basis of clinical practice (40th ed.). London: Churchill Livingstone. ISBN 978-0-8089-2371-8.

[29] Ort V, Bogart BI (2007). Elsevier's integrated anatomy and embryology. Philadelphia, Pa.: Elsevier Saunders. ISBN 978-1-4160-3165-9.

[30] Chung J, Lee YJ, Choi YJ, Ha EJ, Suh CH, Choi M, Baek JH, Na DG; Korean Society of Thyroid Radiology (KSThR); Korean Society of Radiology. Clinical applications of Doppler ultrasonography for thyroid disease: consensus statement by the Korean Society of Thyroid Radiology. Ultrasonography. 2020 Oct;39(4):315-330. doi: 10.14366/usg.20072. Epub 2020 Aug 25. PMID: 32892523; PMCID: PMC7515666.

[31] Iared W, Shigueoka DC, Cristofoli JC, Andriolo R, Atallah AN, Ajzen SA, et al. Use of color Doppler ultrasonography for the prediction of malignancy in follicular thyroid neoplasms: systematic review and meta-analysis. J Ultrasound Med. 2010;29:419–425.

[32] Hahn SY, Shin JH, Na DG, Ha EJ, Ahn HS, Lim HK, et al. Ethanol ablation of the thyroid nodules: 2018 consensus statement by the Korean Society of Thyroid Radiology. Korean J Radiol. 2019;20:609–620.

[33] Kim JH, Baek JH, Lim HK, Ahn HS, Baek SM, Choi YJ, et al. 2017 Thyroid radiofrequency ablation guideline: Korean Society of Thyroid Radiology. Korean J Radiol. 2018;19:632–655.

[34] Lee YH, Baek JH, Jung SL, Kwak JY, Kim JH, Shin JH, et al. Ultrasound-guided fine needle aspiration of thyroid nodules: a consensus statement by the Korean Society of Thyroid Radiology. Korean J Radiol. 2015;16:391–401.

[35] Na DG, Baek JH, Jung SL, Kim JH, Sung JY, Kim KS, et al. Core needle biopsy of the thyroid: 2016 consensus statement and recommendations from Korean Society of Thyroid Radiology. Korean J Radiol. 2017;18:217–237.

[36] Na DG, Lee JH, Jung SL, Kim JH, Sung JY, Shin JH, et al. Radiofrequency ablation of benign thyroid nodules and recurrent thyroid cancers: consensus statement and recommendations. Korean J Radiol. 2012;13:117–125.

[37] Shin JH, Baek JH, Chung J, Ha EJ, Kim JH, Lee YH, et al. Ultrasonography diagnosis and imaging-based management of thyroid nodules: revised Korean Society of Thyroid Radiology consensus statement and recommendations. Korean J Radiol. 2016;17:370–395.

[38] Pearce EN, Farwell AP, Braverman LE. Thyroiditis. N Engl J Med. 2003;348:2646–2655.

[39] Raber W, Gessl A, Nowotny P, Vierhapper H. Thyroid ultrasound versus antithyroid peroxidase antibody determination: a cohort study of four hundred fifty-one subjects. Thyroid. 2002;12:725–731.

[40] Rosario PW, Bessa B, Valadao MM, Purisch S. Natural history of mild subclinical hypothyroidism: prognostic value of ultrasound. Thyroid. 2009;19:9–12.

[41] Park AY, Seo BK. Up-to-date Doppler techniques for breast tumor vascularity: superb microvascular imaging and contrast-enhanced ultrasound. Ultrasonography. 2018;37:98–106.

[42] Rausch P, Nowels K, Jeffrey RB., Jr Ultrasonographically guided thyroid biopsy: a review with emphasis on technique. J Ultrasound Med. 2001;20:79–85.

[43] Darvish L, Khezri M, Teshnizi SH, Roozbeh N, Dehkordi JG, Amraee A. Color Doppler ultrasonography diagnostic value in detection of malignant nodules in cysts with pathologically proven thyroid malignancy: a systematic review and meta-analysis.

[44] Papini E, Guglielmi R, Bianchini A, Crescenzi A, Taccogna S, Nardi F, et al. Risk of malignancy in nonpalpable thyroid nodules: predictive value of ultrasound and color-Doppler features. J Clin Endocrinol Metab. 2002;87:1941–1946.

[45] Deng SH, Jiang Q, Zhu YC, Zhang Y. An analysis of the clinical value of high-frequency color Doppler ultrasound in the differential diagnosis of benign and malignant thyroid nodules. Int J Clin Exp Med. 2018;11:2331–2336.

[46] Salehi M, Nalaini F, Izadi B, Setayeshi K, Rezaei M, Naseri SN. Grayscale vs. color doppler ultrasound in cold thyroid nodules. Glob J Health Sci. 2014;7:147–152.

[47] Hong YR, Wu YL, Luo ZY, Wu NB, Liu XM. Impact of nodular size on the predictive values of gray-scale, color-Doppler ultrasound, and sonoelastography for assessment of thyroid nodules. J Zhejiang Univ Sci B. 2012;13:707–716.

[48] Palaniappan MK, Aiyappan SK, Ranga U. Role of gray scale, color Doppler and spectral Doppler in differentiation between malignant and benign thyroid nodules. J Clin Diagn Res. 2016;10:TC01–TC06.

[49] Chammas MC, Gerhard R, de Oliveira IR, Widman A, de Barros N, Durazzo M, et al. Thyroid nodules: evaluation with power Doppler and duplex Doppler ultrasound. Otolaryngol Head Neck Surg. 2005;132:874–882.

[50] Cerbone G, Spiezia S, Colao A, Di Sarno A, Assanti AP, Lucci R, et al. Power Doppler improves the diagnostic accuracy of color Doppler ultrasonography in cold thyroid nodules: follow-up results. Horm Res. 1999;52:19–24.

[51] Holden A. The role of colour and duplex Doppler ultrasound in the assessment of thyroid nodules. Australas Radiol. 1995;39:343–349.

[52] Moon WJ, Jung SL, Lee JH, Na DG, Baek JH, Lee YH, et al. Benign and malignant thyroid nodules: US differentiation: multicenter retrospective study. Radiology. 2008;247:762–770.

[53] Busilacchi P, Draghi F, Preda L, Ferranti C. Has color Doppler a role in the evaluation of mammary lesions? J Ultrasound. 2012 Jun;15(2):93-8. doi: 10.1016/j.jus.2012.02.007. Epub 2012 Mar 14. PMID: 23396684; PMCID: PMC3558232.

[54] Park AY, Seo BK. Up-to-date Doppler techniques for breast tumor vascularity: superb microvascular imaging and contrast-enhanced ultrasound. Ultrasonography. 2018 Apr;37(2):98-106. doi: 10.14366/usg.17043. Epub 2017 Aug 19. PMID: 29025210; PMCID: PMC5885476.

[55] Park AY, Seo BK, Cha SH, Yeom SK, Lee SW, Chung HH. An innovative ultrasound technique for evaluation of tumor vascularity in breast cancers: superb micro-vascular imaging. J Breast Cancer. 2016;19:210–213.

[56] Ma Y, Li G, Li J, Ren WD. The diagnostic value of superb microvascular imaging (SMI) in detecting blood flow signals of breast lesions: a preliminary study comparing SMI to color Doppler flow imaging. Medicine (Baltimore) 2015;94:e1502.

[57] Yongfeng Z, Ping Z, Wengang L, Yang S, Shuangming T. Application of a novel microvascular imaging technique in breast lesion evaluation. Ultrasound Med Biol. 2016;42:2097–2105.

[58] Zhan J, Diao XH, Jin JM, Chen L, Chen Y. Superb microvascular imaging: a new vascular detecting ultrasonographic technique for avascular breast masses: a preliminary study. Eur J Radiol. 2016;85:915–921.

[59] Ma Y, Li J, Ren W, Deng L. Correlation between superb microvascular imaging and pathological microvessel density in breast tumors. Xiangya Med. 2016;1:30.

www.mindray.com

P/N: ENG-Ultrasound Micro-Angiography (UMA)in the Prostate,Thyroid, and Breast White Paper-210285X20P-20240719

mindray
healthcare within reach